

Elastic Context: Encoding Elasticity for Data-driven Models of Textiles

Alberta Longhini¹, Marco Moletta¹, Alfredo Reichlin¹, Michael C. Welle¹, Alexander Kravberg¹,
Yufei Wang², David Held², Zackory Erickson², and Danica Kragic¹

Abstract—Physical interaction with textiles, such as assistive dressing or household tasks, requires advanced dexterous skills. The complexity of textile behavior during stretching and pulling is influenced by the material properties of the yarn and by the textile’s construction technique, which are often unknown in real-world settings. Moreover, identification of physical properties of textiles through sensing commonly available on robotic platforms remains an open problem. To address this, we introduce Elastic Context (EC), a method to encode the elasticity of textiles using stress-strain curves adapted from textile engineering for robotic applications. We employ EC to learn generalized elastic behaviors of textiles and examine the effect of EC dimension on accurate force modeling of real-world non-linear elastic behaviors.

I. INTRODUCTION

Manipulation of deformable objects such as textiles is common in medical robotics [1], human-robot interaction [2], automation of household tasks [3], assistive dressing [4], [5]. However, as discussed in [6], textile objects are challenging when it comes to manipulation due to complex dynamics and often unknown physical properties (e.g. elasticity, friction, density distribution). These properties depend on the yarn material and textile construction technique and may be difficult to estimate in online robotics manipulation scenarios [7].

We address the problem of encoding elastic properties of textile objects, to learn data-driven models that generalize to variations of elastic properties, see Fig. 1. Modeling the elastic behavior of textiles has been addressed in two rather distant communities: textile engineering [8] and computer graphics [9], [10]. The analytical models from these communities are computationally expensive and commonly not applicable in real-time robotic manipulation. Moreover, such models build on parameters measured with high-precision devices under controlled experiments [11], [12]. Today, there are no commonly adopted and annotated datasets for which these parameters are provided, requiring thus alternative strategies to encode elastic properties of textiles.

Our previous work introduced a taxonomy considering the yarn material and construction techniques [13] to understanding textile properties. It relied on the physical interactions (pulling and twisting) and force-torque measurements. We build upon this work and encode elastic behaviors of textiles through Elastic Context (EC). To formulate the Elastic Context (EC) we draw inspiration from industrial

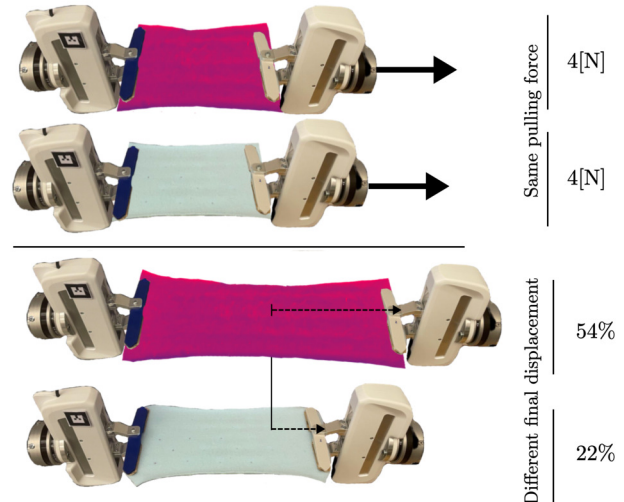


Fig. 1: The role of elasticity in the manipulation of different textile samples, exhibiting different behaviors under the same pulling force.

techniques to characterize textiles, namely the stress-strain curve [14]. These curves can be obtained by recording the forces perceived by a robot when manipulating different textiles. Additionally, we introduce the use of the EC to condition Graph Neural Networks (GNNs) to model the behaviors of textiles with different elastic properties.

We evaluate experimentally the EC and the conditioned GNN on synthetic data obtained in the PyBullet simulator [15], demonstrating the ability of our approach to encode the complex elastic behavior of a wide range of textile. Furthermore, with force measurements collected on two Franka-Emika Panda robots interacting with textiles, we show that increasing the dimensionality of the EC plays an important role in accurately modeling the complex behaviors of textiles when an interactive scenario is considered. Finally, we briefly discuss the limitations of current hardware setups for sensing textile physical properties that go beyond elasticity. In summary, our contributions are:

- *Elastic Context*: a way of encoding elastic properties of textiles suitable for robotic manipulation tasks;
- A detailed experimental evaluation demonstrating, both in simulation and the real world, that EC outperforms methods that do not consider elastic properties when modeling linear and non-linear elastic behaviors of textile.

¹The authors are with the Robotics, Perception and Learning Lab, EECS, at KTH Royal Institute of Technology, Stockholm, Sweden [albertal](mailto:albertal@kth.se), [moletta](mailto:moletta@kth.se), [alfrei](mailto:alfrei@kth.se), [mwelle](mailto:mwelle@kth.se), [okr](mailto:okr@kth.se), [dani](mailto:dani@kth.se)

²The authors are with Carnegie Mellon University, Pittsburgh, USA [yufeiw2](mailto:yufeiw2@cmu.edu), [dheld](mailto:dheld@cmu.edu), [zerickso](mailto:zerickso@andrew.cmu.edu)

II. BACKGROUND

Physical properties of textiles like elasticity, surface friction, and flexibility are determined by the yarn material and the construction technique [16]. Common yarn materials are cotton, wool, or polyester. In modern textiles, these raw materials are blended with elastomers, such as elastane, making the yarn more flexible [17]. The construction technique (woven or knitted) determines how the yarn threads are interlaced or interloped; see our taxonomy in [13]. Woven textiles, such as jeans, are produced with two sets of tightly interlaced yarns that make the textile rather rigid. Knitted textiles instead, are made with one interloped thread and loops that generate space between parallel running threads, resulting in a stretchable textile. These properties play a fundamental role on the interaction dynamics involved in the robotic manipulation of textiles, which can be characterized by the deformation of the textile when an external force, also called stress, is applied [18].

In particular, these interactions might come either from robot actions, such as stretching or shearing the object, or they could be due to collisions with external objects, like the body of a person in an assistive dressing scenario. In both cases, we can reason about the interaction dynamics by identifying three different stages as shown in in Fig. 2. In the first stage (*free* manipulation), no stress is involved during the manipulation as the deformable nature of the textile makes it compliant with the robot’s movement or external objects. In the second phase (*stress* manipulation), the textile starts to induce forces on the end-effector and its elastic properties become relevant to characterize the interaction dynamics of the manipulation. Finally, after a certain force known as rupture force, the textile breaks. Often in robotic tasks, objects are manipulated within the *free* manipulation phase. Nevertheless, precise modeling of the *stress* manipulation phase can be useful for applications requiring a constraint over the forces exerted on the deformable object or to assure that a specific action is correctly performed [2], [6]. So far, these tasks have been studied with the implicit assumption that the elasticity of different manipulated samples do not exhibit large variations in their dynamics, despite the wide diversity of real-world elastic textiles, such as first-aid bandages, t-shirts, jeans.

The complexity of the tasks robots will be faced with in domestic and industrial setups that consider textiles will require the ability to identify elastic properties online. In textile engineering, the evaluation of the elastic behavior of textiles is performed through the stress-strain test, where a fixed load is applied to a piece of textile and the percentage of displacement, also called strain, is measured [11], [14]. In robotics, however, we often do not have robots endowed with advanced sensing tools and most of the interaction has historically relied on visual sensing [19]. We need therefore to rely on common force-torque sensors to define suitable alternative to the stress-strain test. In this work we propose the EC, a way of encoding elastic behavior of textiles that can be obtained from the classical robot sensing and

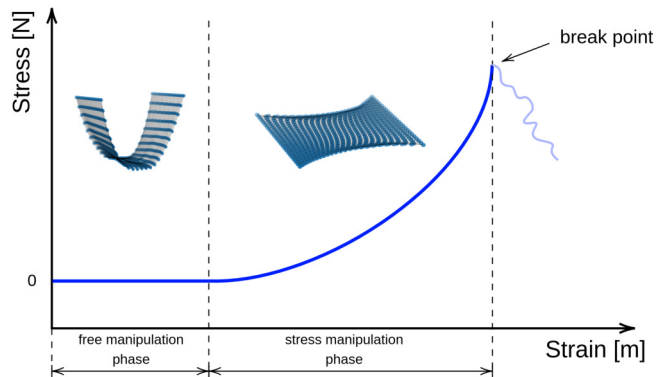


Fig. 2: Typical stress curve for manipulation of elastic textiles, categorised in three stages: *free* manipulation, *stress* manipulation and break point. More details in text.

can be leveraged by a data driven model to generalize its performances on a wide range of textiles with different elastic properties.

III. RELATED WORK

In this section, we review related work regarding elasticity of textiles from both the analytical and data-driven perspective. Recent reviews provide an overview of deformable objects, including textiles, and their use in dexterous robotic manipulation [20], [21].

A. Analytical Models of Elasticity in Textiles

Analytical models of textiles usually rely on physics-based modeling and geometric representations, such as particles or graphs [21]. Position-based Dynamics (PBDs) approaches model the displacements of a discrete system of particles by applying geometrical constraints [18]. This strategy is computationally efficient but struggles to model net forces and is resolution dependent [11]. Graph models overcome these problems by encoding the interaction between the particles in the edges of the graph. In mass-spring models, the edges represent springs following Hooke’s law to encode linear elastic relationship [22]. Damping, bending, and shearing factors can be integrated to reproduce more complex behaviors. However, linear approximations of the textile dynamics underperform with large deformations. The high-strain regime cannot be ignored when modeling textiles as such deformations may occur near the garment’s seams or when parts of the textile are physically constrained. Non-linear models, such as the Neo Hookean or the St. Venant–Kirchhoff, have the advantage of being more accurate than the mass-spring models, but their computational complexity is not suitable for real-time simulations [9], [23], [24]. In robotic manipulation tasks, task-specific and low-dimensional textile representations are often favored over a precise description of all possible mechanical behaviors of the textiles [25]. Finding a suitable trade-off between the model accuracy and numerical efficiency is therefore of fundamental importance [26].

B. Data-driven Models of Textiles

A limitation of analytical models is the requirement of having precise knowledge of the physical properties of the textile, as these properties are often unknown in real-world scenarios. Despite the effort to simplify the complex measurement tools used in textile engineering, the estimation of textile properties remains highly engineered [22], [27]. Black-box models like neural networks provide a viable solution to model dynamic behavior without explicit knowledge of all the properties. GNNs have shown to be a suitable framework in the context of learning graph-based dynamics, being employed in a variety of complex domains including deformable objects [28]–[30]. Battaglia, *et al.* [31] proposed Interaction Networks (INs) to learn a physical engine to capture local interactions among nodes by modeling them through a complete graph. Li *et al.* [32] extended this framework by proposing Propagation Networks (PNs), which enable instantaneous propagation of forces by multi-step message passing. These approaches have shown excellent results in modeling deformable objects, but they assume the properties of the object to be known a priori. In this work we relax this assumption suggesting to learn a large variety of elastic behaviors by conditioning a GNN on our proposed *Elastic Context*.

IV. ELASTIC CONTEXT FOR DATA-DRIVEN MODELS

To account for the wide range of possible elastic responses that textiles may have, we learn a graph-based dynamics prediction model using a GNN, which we condition on information about the textile elasticity - *Elastic Context* (EC).

A. Elastic Context

A potential measure of a material’s elasticity is the elastic modulus, which evaluates the material’s resistance to deformation under stress [18]. Its value can be derived by measuring the slope of the stress-strain curve corresponding to a specific material or textile sample. The stress σ is defined as the deformation force F [N] acting on the cross-sectional area A [m²] of the sample, while the strain ϵ corresponds to the percentage of displacement Δl of the sample with respect to its original length l_0 . Using these quantities, the elastic modulus is calculated as $e = \sigma/\epsilon$.

Fig. 3 presents stress-strain curves for two real-world textile samples. The values were obtained from force-feedback readings of the dual-arm robotic setup shown in Fig. 4. The robots were pulling the samples with $l_0 = 0.18$ m and $A = 0.18 \times 10^{-3}$ m² until a stress $\sigma_{max} = 30$ KPa was reached. Fig. 3 indicates how encoding elastic properties of textile with the elastic modulus can only describe small displacements and linear behaviors. We observe that linear approximations can accurately describe the rigid sample (blue line) but loses accuracy for the elastic sample (red line), which increases its rigidity with increasing stress.

To overcome the limitation of the elastic modulus, we define EC as the combination of elastic modules of a given textile evaluated at n_{EC} equidistant points between 0 and σ_{max} on the stress-strain curve, where n_{EC} determines the

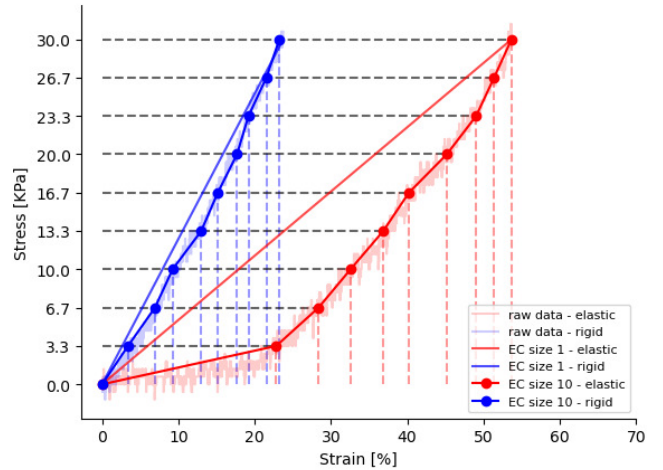


Fig. 3: Stress-strain curves of a rigid (blue) and an elastic (red) textile sample: with $n_{EC} = 1$ we recover the elastic modulus, describing a linear elastic behavior that accurately represents the rigid sample (blue) but not the elastic one (red); with a higher-dimensional EC ($n_{EC} = 10$), we are able to better describe the non-linear behavior of the elastic sample.

dimensionality of the EC. We thus represent the EC as a vector $EC = [e_1, \dots, e_{n_{EC}}] \in \mathbb{R}^{n_{EC}}$, where $e_i = \sigma_i/\epsilon_i$ is the elastic modulus evaluated from the textile stress-strain curve at the corresponding stress σ_i . Since both stress and strain measurements are normalized by the size of the sample, the EC is a consistent definition of elasticity that is comparable between textiles of different sizes as long as σ_{max} is fixed.

B. Graph Model

We propose to represent textiles as graphs, and to learn their dynamics using GNNs [33], [34]. We can thus formulate the problem of learning the force and position dynamics of textiles as learning the parameters θ of a GNN Λ_θ . Specifically, let $G_k = (V_k, E_k)$ be a graph representing a textile sample $k \in K$, where V is the set of nodes, E the set of edges and K is the set of all possible elastic samples. We define the features of each node $v \in V_k$ by their position $x_v^t \in \mathbb{R}^3$ in the Euclidean space at time step t . The edges $e \in E_k$ instead describe the elastic relation between two connected nodes. We propose to define the features of the edges as $EC_k \in \mathbb{R}^{n_{EC}}$ evaluated for the specific elastic textile k . EC is therefore a feature shared among all the edges encoding the elastic property of the textile into G_k .

At time t , a dual arm robotic manipulator grasping the textile applies an action $a^t = \Delta x_{v_{grasp}}^t \in \mathbb{R}^3$ at the grasped nodes $v_{grasp} \in V_k$, resulting in new positions x_v^{t+1} of the nodes and a textile specific force F_k^{t+1} perceived at the end-effectors. Our goal is to learn a model that leverages the EC to predict x_v^{t+1} and F_k^{t+1} , given the initial state of G_k^t and the action a^t applied to the textile.

We employ a standard message-passing architecture for the GNN model Λ_θ [32]. The input graph is constructed by first concatenating the action to the features of the grasped nodes.

The features of both nodes and edges are then projected into latent representations, respectively h_0 and c , through learned encoders parameterized with a Multi-layer Perceptron (MLP). Subsequently, every node aggregates messages from its neighbors via T propagation steps, where each propagation leverages the elastic information embedded into the features of the edges to compute the final update of the features of the nodes. In particular, for the propagation step $\tau \in [1, T]$, the features of each node get updated follows:

$$h_i^\tau = \Phi \left(\sum_{s \in N_i} \Psi (h_i^{\tau-1}, h_s^{\tau-1}, c) \right) \quad \forall v_i \in V_k, \quad (1)$$

where N_i denotes the set of neighbor nodes of node i , Ψ is a message-passing network that propagates the information of each node i to its neighbors, and Φ is an aggregation function of the total information received by each node. We parametrized both Ψ and Φ via separate MLPs. Finally, we encode the features of each node h_i^T to obtain the estimate of the displacement of each node in G_k^{t+1} and the force-feedback F_k^{t+1} perceived by the robot in the next time-step $t+1$. This process is done by two projection heads (MLPs), where the final value of F_k^{t+1} is the result of an average pooling layer. The overall model Λ can be learned using a dataset $\mathcal{D} = \{(G_k^t, G_k^{t+1}, F_k^{t+1}, a_k^t, EC_k)\}_{\forall k \in K}$, optimising the parameters θ using a supervised loss on the prediction of the nodes position and the force exerted at the grasp-nodes:

$$\mathcal{L} = \mathbb{E}_{\mathcal{D}} [d(\Lambda_\theta(G_k^t, a_k^t, EC_k), (G_k^{t+1}, F_k^{t+1}))], \quad (2)$$

where d is a measure of the distance between the prediction and the ground-truth of graphs and forces. In our case, d is implemented as the sum of Mean-Squared Error (MSE) of the graph's position and of the force.

V. EXPERIMENTAL EVALUATION

In this section, we evaluate the performance of the EC in modeling linear and non-linear dynamics of textile objects for robotic manipulation tasks. In particular, we show using simulation that EC with GNNs leads to more accurate force-feedback predictions of unseen elastic textiles. Furthermore, we analyze the role of the dimensionality of EC both in simulation and real-world scenarios, highlighting the importance of increasing the EC size (n_{EC}) in presence of non-linear force dynamics.

A. Experimental Setup

Task: We evaluate the performance of EC in predicting forces perceived by a robot when manipulating *unseen* elastic samples. To this end, we devised a two-stage simplified assistive dressing task. In the first stage, a dual-arm robot is tasked to stretch a textile up to a maximum stress $\sigma_{max} = 3 \times 10^4$ Pa, corresponding to a $F_{max} = \sigma_{max} \times A_0$ [N] force perceived at the end-effector for a textile with cross-sectional area A_0 [m²]. The forces recorded during this interaction are used to recover the EC, following the procedure defined in Section IV. In the second stage, the same dual-arm robot is tasked with pulling the sample over a sphere, resembling the head of a person, up to a cumulative gripper displacement of a_{max}

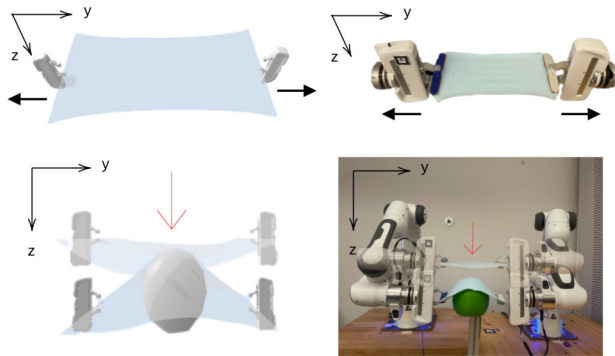


Fig. 4: Simulated (left) and real-world (right) environments to instantiate the simplified assistive dressing task: the y -axis corresponds to the pulling direction used to collect the context, while the z -axis is related to the task execution.

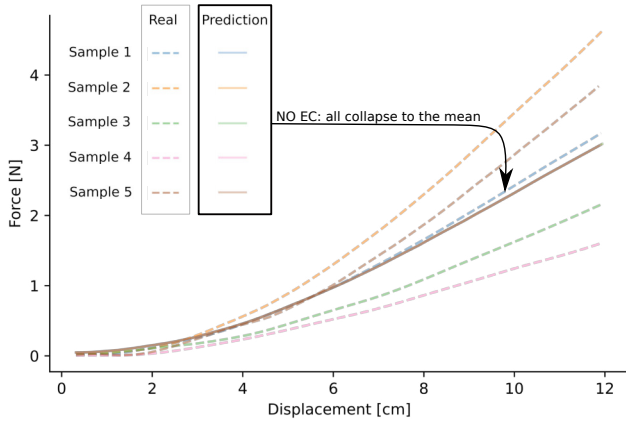
[cm] from the instant the textile starts to induce force on the end-effector.

The goal of our model is to perform a *force-forecasting* task, which consists of predicting the force response of the textile from the moment of contact with the object until the goal displacement is reached. We reproduced the aforementioned scenario both in the real world and in the PyBullet simulator [15], [35]. An overview of the setup is presented in Fig. 4, where two robotic grippers either stretch a piece of textile (to obtain the EC) or pull it over a rigid sphere (simplified assistive dressing scenario). To manipulate the textile in the real-world setting we used two Franka-Emika Panda equipped with Optoforce Force/Torque sensors, while in the simulation we only used free-floating end-effectors and their force sensors.

Data Collection: The simulation dataset $\mathcal{D}_{SIM} = \{(G_k^t, G_k^{t+1}, F_k^{t+1}, a_k^t, EC_k)\}_{k \in K}$ was collected performing the aforementioned task with parameters $A_0 = 0.18 \times 10^{-3}$ m² and $l_0 = 0.18$ cm. For each execution, we varied the elastic properties $k \in K$ of the simulated textile. $K = [20, 119]$ was defined empirically by selecting the *elasticity* object parameter to avoid unstable behaviors of the mesh during the collision with the sphere. We uniformly sampled k with a step size of 1 while keeping the *bending* and *damping* properties fixed to 0.1 and 1.5 respectively, obtaining a total of 100 different elastic samples.

The ground truth forces used to obtain EC_k and F_k^{t+1} were recorded from the force sensors on the virtual grippers. We smoothed the force measurements using a Savitzky-Golay filter [36] with a window size of 21 and a third-grade polynomial to account for noisy measurements due to collision interactions. We obtained G_k^t and G_k^{t+1} by accessing the ground truth positions of all textile vertices disposed as a 25×25 3D mesh, which we subsequently downsampled to 12×12 . The gripper actions a_k^t are sequences of 33 displacements along the z -axis in the interval of $[0, a_{max}]$, where $a_{max} = 12$ cm, providing a total of 3300 data samples.

For the real-world experiments, where the focus is on analysing the role of the EC for non-linear force dynamics, we collected a dataset $\mathcal{D}_{RW} = \{(F_k^{t+1}, a_k^t, EC_k)\}_{k \in K}$. We leave



(a) Baseline

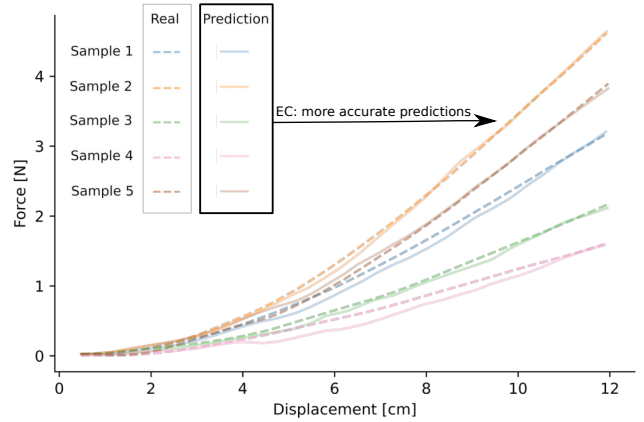
(b) GNN + EC ($n_{EC} = 1$)

Fig. 5: Force-forecasting predictions of the baseline model (a) and the GNNs + EC with dimension $n_{EC} = 1$ model (b) evaluated on 5 test elastic samples. The results show that the GNN + EC model generalizes to unseen elastic textiles, leveraging the information provided by the EC.

the collection of the real-world ground-truth graphs G_k^t and G_k^{t+1} for future work, which could be performed leveraging recent approaches for state estimation and dynamics prediction for cloth [30], [37]. Differently from the simulated data, the ground truth elastic properties of the textile are not easily accessible as their estimation would require specific tensile tests as discussed in Section II. To overcome this challenge, we fixed K according to a proxy categorization of textile properties represented by the taxonomy proposed in [13]. We chose 40 different combinations of yarn material to maximize the variance of the elastic responses, while keeping the construction technique fixed to knitted as the one leading to more elastic behaviors. In particular, we chose the following textile samples classified by their materials: 8 wool, 18 cotton and 10 polyester. Cotton and polyester material classes contain samples with different percentages of elastane.

GNN Implementation: To evaluate the role of the EC, we instantiate a GNN with node and edge encoders composed of two linear layers with 16 neurons each. The message-passing and aggregation functions are implemented as two linear layers with 16 neurons and $T = 8$. The graph prediction and force prediction heads consist of two linear layers with 16 hidden neurons respectively. We used the Rectified Linear Units (ReLU) [38] as activation function and layer normalization throughout the network except at the final layers of each block [39]. We train the GNN for 2000 epochs, with a batch size of 32, and a learning rate of 3×10^{-4} . We randomly split the 3300 data points from simulation with a 0.2 test-train split, ensuring that the elastic behaviors in the test set are unseen. The parameters were optimized using Adam [40]. Both the training objective and test evaluation metric of the models are the Mean Squared Error (MSE) between the model’s force prediction and the ground truth.

B. Elastic Context Evaluation

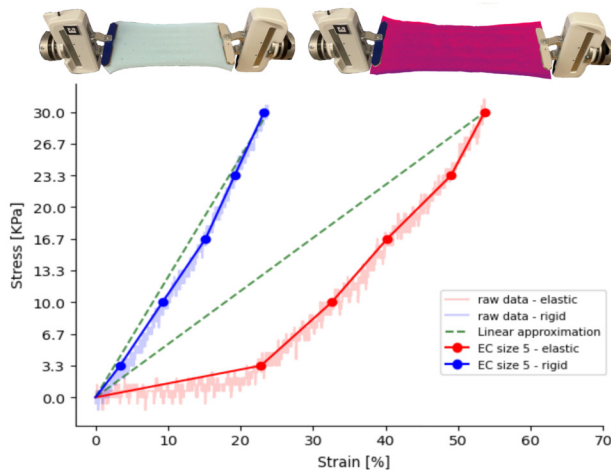
We start by evaluating the role of the Elastic Context in the simulation environment, as the ground truth properties

of the underlying model of the textile are easily accessible. We carry out the evaluation on the *force-forecasting* task, where the goal is to predict the force evolution and the state (represented as a graph) of unseen elastic textiles up to the goal displacement of 12 cm. We compare our proposed GNN informed with the EC to a *baseline* GNN that has no EC information, and to an *oracle* GNN that has access to the ground truth properties of the textile. Furthermore, we evaluate the effect the size of the EC has on simulated force dynamics, where we considered $n_{EC} = \{1, 2, 5\}$.

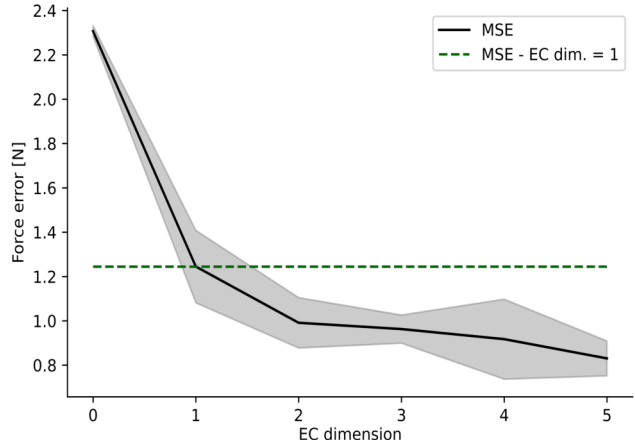
Table I presents the test MSE of the force and graph rollout predictions evaluated on 20 *unseen* elastic samples. Regarding the force prediction, the results demonstrate that the baseline model performs worse than the GNNs that have access to elastic information. Moreover, the models that use the EC have comparable performances to the oracle, showing that EC enables the models to leverage elastic information. These findings are further supported by the qualitative results of the *force forecasting* prediction visualized in Fig. 5. The baseline model (Fig. 5a) predicts the same force evolution for all test samples, while the GNN with EC $n_{EC} = 1$ (Fig. 5b) successfully covers a larger spectrum of the test set, improving the accuracy of the predictions of different elastic behaviors. These results confirm the relevance of encoding elastic behavior of textiles, such as the EC, especially for real-world applications requiring a constraint over the forces exerted on the deformable object (e.g., assistive dressing or

TABLE I: Mean and standard deviation of the MSE of the *force-forecasting* task rollout evaluated on 20 different test samples.

Model	FORCE error [N]	GRAPH error [m]
Oracle	0.207 ± 0.239	0.885 ± 0.301
Baseline	3.169 ± 2.434	0.921 ± 0.292
GNN $n_{EC} = 1$	0.269 ± 0.301	0.896 ± 0.234
GNN $n_{EC} = 2$	0.235 ± 0.108	1.108 ± 0.411
GNN $n_{EC} = 5$	0.246 ± 0.247	1.206 ± 0.409



(a) Real-world force profiles



(b) Role of the EC dimension in real world

Fig. 6: (a) Real world force profiles of respectively a rigid sample (blue) with an almost linear behavior, and an elastic sample (red) exhibiting a non-linear behavior. (b) *Force forecasting* MSE of the MLP models tested on 8 *unseen* real-world samples. Results averaged over 6 randomly-seeded runs.

bathing assistance). Furthermore, we observe from Table I that increasing the size of the EC does not lead to improvements in the model performance, suggesting that $n_{EC} = 1$ is enough to describe the variety of simulated elastic behaviors that assume a linear force dynamics.

Regarding the graph predictions, the quantitative results of the evaluated models are presented in Table I. It can be noticed that all the models perform comparably, reflecting our design choices of using displacements as actions in combination with textiles with *isotropic* elastic properties. In this scenario, the displacement of the nodes depends solely on the action applied by the robot, which is an information available to all the models. The same consideration does not hold if we consider textiles with anisotropic elastic properties, which represent an interesting future direction to explore.

C. Real-world Evaluation

In this section we showcase the relevance of increasing the dimensionality of EC in the presence of non-linear force dynamics. In particular, our goal is to highlight that an EC of dimension 1 represents a good approximation of linear force behaviors, but it loses accuracy for non-linear real-world behaviors as highlighted in Fig. 6a. To fulfill this goal, we implemented an MLP with two hidden layers of 8 units each and ReLU as the activation function, and we trained it with the real-world dataset \mathcal{D}_{RW} to predict F_k^{t+1} given a_k^t and EC_k . We trained different variants of the model by choosing the dimensionality of the EC in the range $n_{EC} \in [0, 5]$, where each of the variants is trained for 1k epochs. Fig. 6b presents the force prediction MSE of each model on 8 test elastic samples averaged over 6 randomly-selected seeds, where the test samples were randomly selected from the dataset for each seed. Contrarily to what observed for the simulation experiments, these results show that increasing the dimensionality of the EC leads to more accurate predictions

of real-world non-linear force profiles with the respect to the models trained with an EC with dimension equal to 1 (dashed line). This outcome highlights the gap between simulated and real-world force dynamics. An interesting future research direction to explore is how this gap hinders the model performance when trained using simulated data and then directly applied to real-world textiles. We plan to investigate this question in our future work and to address the problem of how to bridge the gap between simulation and real world for better sim-to-real transfer for deformable object manipulation.

VI. CONCLUSIONS

In this work, we presented and evaluated *Elastic Context* (EC), an approach to encode elasticity in data-driven models of textiles. We have shown the role of the EC in a *force forecasting* prediction task on both simulated and real world data. The EC can be easily employed in real-world robotic platforms, providing a simple way to understand elastic properties of textiles in scenarios where no labels are provided. Such understanding can be of great importance in assistive robotics and human-robot interaction, where the manipulation of textile and other deformable objects is considered. The proposed EC is suitable for describing elastic properties, while factors influencing manipulation of textiles go beyond the non-linear elastic behaviors, like for example friction and flexibility affecting tasks such as ironing or folding. Furthermore, interesting aspects to study may be the breaking point of textiles or changing properties when textiles are covered with substances like water or oil. All these open new research avenues for the future.

VII. ACKNOWLEDGEMENTS

This work has been supported by the European Research Council (ERC-BIRD), Swedish Research Council and Knut and Alice Wallenberg Foundation.

REFERENCES

- [1] B. S. Peters, P. R. Armijo, C. Krause, S. A. Choudhury, and D. Oleynikov, "Review of emerging surgical robotic technology," *Surgical endoscopy*, vol. 32, no. 4, pp. 1636–1655, 2018.
- [2] Z. Erickson, H. M. Clever, G. Turk, C. K. Liu, and C. C. Kemp, "Deep haptic model predictive control for robot-assisted dressing," in *2018 IEEE international conference on robotics and automation (ICRA)*. IEEE, 2018, pp. 4437–4444.
- [3] A. Verleysen, M. Biondina, and F. Wyffels, "Video dataset of human demonstrations of folding clothing for robotic folding," *The International Journal of Robotics Research*, vol. 39, no. 9, pp. 1031–1036, 2020.
- [4] S. D. Klee, B. Q. Ferreira, R. Silva, J. P. Costeira, F. S. Melo, and M. Veloso, "Personalized assistance for dressing users," in *International Conference on Social Robotics*. Springer, 2015, pp. 359–369.
- [5] A. Kapusta, Z. Erickson, H. M. Clever, W. Yu, C. K. Liu, G. Turk, and C. C. Kemp, "Personalized collaborative plans for robot-assisted dressing via optimization and simulation," *Autonomous Robots*, vol. 43, no. 8, pp. 2183–2207, 2019.
- [6] C. Chi, B. Burchfiel, E. Cousineau, S. Feng, and S. Song, "Iterative residual policy: for goal-conditioned dynamic manipulation of deformable objects," *arXiv preprint arXiv:2203.00663*, 2022.
- [7] H. Ha and S. Song, "Flingbot: The unreasonable effectiveness of dynamic manipulation for cloth unfolding," in *Conference on Robot Learning*. PMLR, 2022, pp. 24–33.
- [8] S. Poincloux, M. Adda-Bedia, and F. Lechenault, "Geometry and elasticity of a knitted fabric," *Physical Review X*, vol. 8, no. 2, p. 021075, 2018.
- [9] D. Clyde, J. Teran, and R. Tamstorf, "Modeling and data-driven parameter estimation for woven fabrics," in *Proceedings of the ACM SIGGRAPH/Eurographics Symposium on Computer Animation*, 2017, pp. 1–11.
- [10] G. Sperl, R. Narain, and C. Wojtan, "Homogenized yarn-level cloth," *ACM Trans. Graph.*, vol. 39, no. 4, p. 48, 2020.
- [11] B. Eberhardt, A. Weber, and W. Strasser, "A fast, flexible, particle-system model for cloth draping," *IEEE Computer Graphics and Applications*, vol. 16, no. 5, pp. 52–59, 1996.
- [12] M. I. Yousef and G. K. Stylios, "Investigating the challenges of measuring combination mechanics in textile fabrics," *Textile Research Journal*, vol. 88, no. 23, pp. 2741–2754, 2018.
- [13] A. Longhini, M. C. Welle, I. Mitsioni, and D. Kragic, "Textile taxonomy and classification using pulling and twisting," *arXiv preprint arXiv:2103.09555*, 2021.
- [14] S. Kawabata and M. Niwa, "Fabric performance in clothing and clothing manufacture," *Journal of the Textile Institute*, vol. 80, no. 1, pp. 19–50, 1989.
- [15] E. Coumans and Y. Bai, "Pybullet, a python module for physics simulation for games, robotics and machine learning," <http://pybullet.org>, 2016–2021.
- [16] S. Grishanov, "Structure and properties of textile materials," in *Handbook of textile and industrial dyeing*. Elsevier, 2011, pp. 28–63.
- [17] S. Uyanik and K. H. Kaynak, "Strength, fatigue and bagging properties of plated plain knitted fabrics containing different rates of elastane," *International Journal of Clothing Science and Technology*, 2019.
- [18] V. E. Arriola-Rios, P. Guler, F. Ficuciello, D. Kragic, B. Siciliano, and J. L. Wyatt, "Modeling of deformable objects for robotic manipulation: A tutorial and review," *Frontiers in Robotics and AI*, p. 82, 2020.
- [19] D. Kragić, L. Petersson, and H. I. Christensen, "Visually guided manipulation tasks," *Robotics and Autonomous Systems*, vol. 40, no. 2-3, pp. 193–203, 2002.
- [20] Y. C. Hou, K. S. M. Sahari, and D. N. T. How, "A review on modeling of flexible deformable object for dexterous robotic manipulation," *International Journal of Advanced Robotic Systems*, vol. 16, no. 3, p. 1729881419848894, 2019.
- [21] H. Yin, A. Varava, and D. Kragic, "Modeling, learning, perception, and control methods for deformable object manipulation," *Science Robotics*, vol. 6, no. 54, 2021.
- [22] H. Wang, J. F. O'Brien, and R. Ramamoorthi, "Data-driven elastic models for cloth: modeling and measurement," *ACM transactions on graphics (TOG)*, vol. 30, no. 4, pp. 1–12, 2011.
- [23] P. Boonvisut and M. C. Çavuşoğlu, "Estimation of soft tissue mechanical parameters from robotic manipulation data," *IEEE/ASME Transactions on Mechatronics*, vol. 18, no. 5, pp. 1602–1611, 2012.
- [24] E. Miguel, D. Miraut, and M. A. Otaduy, "Modeling and estimation of energy-based hyperelastic objects," in *Computer Graphics Forum*, vol. 35, no. 2. Wiley Online Library, 2016, pp. 385–396.
- [25] D. McConachie, M. Ruan, and D. Berenson, "Interleaving planning and control for deformable object manipulation," in *Robotics Research*. Springer, 2020, pp. 1019–1036.
- [26] D. Marinkovic and M. Zehn, "Survey of finite element method-based real-time simulations," *Applied Sciences*, vol. 9, no. 14, p. 2775, 2019.
- [27] E. Miguel, D. Bradley, B. Thomaszewski, B. Bickel, W. Matusik, M. A. Otaduy, and S. Marschner, "Data-driven estimation of cloth simulation models," in *Computer Graphics Forum*, vol. 31, no. 2pt2. Wiley Online Library, 2012, pp. 519–528.
- [28] S. Georgousis, M. P. Kenning, and X. Xie, "Graph deep learning: State of the art and challenges," *IEEE Access*, 2021.
- [29] M. B. Chang, T. Ullman, A. Torralba, and J. B. Tenenbaum, "A compositional object-based approach to learning physical dynamics," *arXiv preprint arXiv:1612.00341*, 2016.
- [30] X. Lin, Y. Wang, Z. Huang, and D. Held, "Learning visible connectivity dynamics for cloth smoothing," in *Conference on Robot Learning*. PMLR, 2022, pp. 256–266.
- [31] P. W. Battaglia, R. Pascanu, M. Lai, D. Rezende, and K. Kavukcuoglu, "Interaction networks for learning about objects, relations and physics," *arXiv preprint arXiv:1612.00222*, 2016.
- [32] Y. Li, J. Wu, J.-Y. Zhu, J. B. Tenenbaum, A. Torralba, and R. Tedrake, "Propagation networks for model-based control under partial observation," in *2019 International Conference on Robotics and Automation (ICRA)*. IEEE, 2019, pp. 1205–1211.
- [33] T. N. Kipf and M. Welling, "Semi-supervised classification with graph convolutional networks," *arXiv preprint arXiv:1609.02907*, 2016.
- [34] A. Sanchez-Gonzalez, J. Godwin, T. Pfaff, R. Ying, J. Leskovec, and P. Battaglia, "Learning to simulate complex physics with graph networks," in *International Conference on Machine Learning*. PMLR, 2020, pp. 8459–8468.
- [35] Z. Erickson, V. Gangaram, A. Kapusta, C. K. Liu, and C. C. Kemp, "Assistive gym: A physics simulation framework for assistive robotics," in *2020 IEEE International Conference on Robotics and Automation (ICRA)*. IEEE, 2020, pp. 10169–10176.
- [36] A. Savitzky and M. J. Golay, "Smoothing and differentiation of data by simplified least squares procedures," *Analytical chemistry*, vol. 36, no. 8, pp. 1627–1639, 1964.
- [37] Z. Huang, X. Lin, and D. Held, "Mesh-based dynamics with occlusion reasoning for cloth manipulation," *arXiv preprint arXiv:2206.02881*, 2022.
- [38] A. F. Agarap, "Deep learning using rectified linear units (relu)," *arXiv preprint arXiv:1803.08375*, 2018.
- [39] J. L. Ba, J. R. Kiros, and G. E. Hinton, "Layer normalization," *arXiv preprint arXiv:1607.06450*, 2016.
- [40] D. P. Kingma and J. Ba, "Adam: A method for stochastic optimization," *arXiv preprint arXiv:1412.6980*, 2014.